Int. J. Heat Mass Transfer. Vol. 36, No. 6, pp. 1701–1706, 1993
Printed in Great Britain

0017-9310/93 $6.00+0.00
Pergamon Press Ltd

Heat transfer in fully developed turbulent channel flow: comparison between experiment and direct numerical simulations

M. TEITEL and R. A. ANTONIA
Department of Mechanical Engineering, University of Newcastle, N.S.W. 2308, Australia

(*Received* 17 *May* 1991)

Abstract—Measurements in a fully developed turbulent channel flow with one wall heated at constant temperature and the opposite wall at approximately ambient temperature are compared with available direct numerical simulations. The consequences of the different thermal boundary conditions used in the experiment and the simulations are explored, especially with regard to distributions of the turbulent heat flux and the average production of temperature variance. In the near-wall region, the measured mean and r.m.s. temperature distributions are in good agreement with the simulations. Outside this region, differences exist mainly due to differences in the thermal boundary conditions at the opposite wall.

1. INTRODUCTION

KIM *et al.* [1] presented results from a direct numerical simulation of a turbulent channel flow and compared them with existing experimental data at comparable Reynolds numbers. The comparison showed generally good agreement, most of the discrepancies occurring in the immediate vicinity of the wall. More recently, the direct numerical simulation data has been extended to a slightly heated fully developed turbulent channel flow [2–5]. These data have been obtained at approximately the same Reynolds number but for different thermal boundary conditions. For example, the majority of the results published by Kim and Moin [3] were for the case of a passive scalar which was created internally and removed at the two (constant temperature) walls. In Lyons *et al.*'s [4] simulation, one wall was heated while the other was cooled at the same rate. Kasagi *et al.* [5], noting that the conditions used in ref. [3] would be difficult to set up experimentally, carried out a simulation with both walls heated at constant heat flux. While there is little doubt that the above DNS data will prove to be important for testing and developing heat transport models (especially in the region adjacent to the wall), it seems useful to compare these data with experiment. To this purpose, measurements were made in a fully developed turbulent channel flow with one wall heated and the other (opposite) wall maintained at approximately ambient temperature. The Reynolds number was approximately the same as for the simulations. The amount of heating was sufficiently small for temperature to be a passive scalar, as in the simulations.

A second aim of the present paper is to examine the consequences of the slight differences in thermal boundary conditions, as used in the simulations and experiment, on quantities such as the turbulent heat flux $\overline{v^+\theta^+}$ and the average production of the temperature variance $-\overline{v^+\theta^+}(\mathrm{d}\bar{T}^+/\mathrm{d}y^+)$. These consequences are discussed in Section 2. Experimental results (Section 4) include distributions of mean and r.m.s. temperature, $\overline{v^+\theta^+}$ and $-\overline{v^+\theta^+}(\mathrm{d}\bar{T}^+/\mathrm{d}y^+)$. The influence of Reynolds number in the near-wall region is briefly considered.

2. TURBULENT HEAT FLUX DISTRIBUTIONS: EFFECT OF DIFFERENT THERMAL BOUNDARY CONDITIONS

In this section, we briefly consider the implications of different thermal boundary conditions on the variation of the average thermometric heat flux $\overline{v\theta}$ across the channel. It is assumed that the velocity and thermal fields are fully developed. Textbooks on heat transfer (e.g. refs. [6, 7]) define a thermally fully developed flow as one in which the heat transfer coefficient h is constant (with respect to x). From this definition it is easy to show that for a duct with constant heat flux at both walls, the bulk mean temperature T_m increases linearly with x, i.e. $\mathrm{d}T_m/\mathrm{d}x = \text{constant}$. For consistency with a hydrodynamically fully developed flow, where the velocity field is homogeneous in x, we prefer to define a thermally fully developed flow as one where the temperature field is homogeneous in x so that all gradients with respect to x are zero. It is also assumed that the velocity and thermal fields have identical origins. The different thermal boundary conditions that are considered are summarized in the definition sketch of Fig. 1. A constant heat flux q_w (which may be either positive or negative) is applied to the lower wall. A

NOMENCLATURE

C_f skin friction coefficient, $\tau_w/\frac{1}{2}U_0^2$
C_p specific heat at constant pressure
h heat transfer coefficient
k thermal conductivity
Nu Nusselt number, $2\delta h/k = 2St\ Pr\ Re$
Pr molecular Prandtl number, ν/α
Q internal source/sink of constant heat flux
q_w thermometric wall heat flux
Re Reynolds number, $U_0\delta/\nu$
St Stanton number, $q_w/U_0(T_w-T_0)$
$T,\bar{T}$ instantaneous and mean temperatures, respectively
$\bar{T}^+$ $(T_w-\bar{T})/T_\tau$
T_τ friction temperature, q_w/U_τ
T_w wall temperature
T_0 mean temperature on channel centreline
t time
u,v velocity fluctuations in x and y directions, respectively
U_0 centreline velocity
U_τ friction velocity, $\tau_w^{1/2}$
$\overline{v\theta}$ heat flux normal to wall
x,y coordinates: x, streamwise; y, normal to the wall.

Greek symbols
α thermal diffusivity, $k/\rho C_p$
δ channel half-width
δ^+ Reynolds number or Kármán number, $\delta U_\tau/\nu$
θ temperature fluctuation
ν kinematic viscosity
τ_w kinematic wall shear stress.

Subscripts
max maximum value
w wall value
0 centreline value.

Superscripts
′ r.m.s. value
+ normalization by wall variables U_τ, T_τ, ν
− conventional time average.

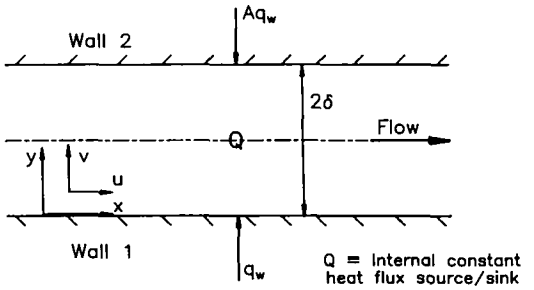

FIG. 1. Schematic arrangement of fully developed channel flow, showing various thermal boundary conditions.

heat flux, equal to Aq_w (where A has variable magnitude and sign) is applied to the opposite wall.

The heat diffusion equation is given by

$$\frac{DT}{Dt} = \alpha\nabla^2 T + Q \tag{1}$$

where Q represents an internal source/sink of constant heat flux.

With the assumption that $d\bar{T}/dx = 0$, the equation for the mean temperature $\bar{T}$ simplifies to

$$\alpha\frac{d^2\bar{T}}{dy^2} - \frac{d(\overline{v\theta})}{dy} + Q = 0 \tag{2}$$

with the boundary conditions

$$\text{(i) at } y = 0,\ \overline{v\theta} = 0,\ -\alpha\frac{d\bar{T}}{dy} = q_w \tag{3a}$$

$$\text{(ii) at } y = 2\delta,\ \overline{v\theta} = 0,\ \alpha\frac{d\bar{T}}{dy} = Aq_w. \tag{3b}$$

An expression for the total heat flux can be obtained by integrating equation (2) with respect to y (from $y = 0$ to 2δ). The resulting expression is

$$Pr^{-1}\frac{d\bar{T}^+}{dy^+} - \overline{v^+\theta^+} = \frac{y^+}{2\delta^+}(A+1) - 1 \tag{4}$$

with the relation between Q and q_w given by

$$Q = -\frac{q_w}{2\delta}(A+1). \tag{5}$$

The superscript + in equation (4) denotes normalization by wall variables, i.e. by the friction velocity U_τ and the friction temperature T_τ† and a length scale ν/U_τ, where ν is the kinematic viscosity of the fluid; Pr ($\equiv \nu/\alpha$) the molecular Prandtl number. For convenience, $\bar{T}$ is taken relative to T_w; the temperature of wall 1, so that $\bar{T}^+ = (T_w-\bar{T})/T_\tau$.

We distinguish between three specific situations.

Case a: $A = -1$

This corresponds to wall 2 being cooled (when $q_w > 0$) at the same rate as wall 1 is heated. It follows from equation (5) that $Q = 0$, i.e. an internal heat source/sink is not required for the flow to be thermally fully developed. The total heat flux is constant, i.e.

† Note that T_τ is negative when q_w is negative.

$$Pr^{-1}\frac{d\bar{T}^+}{dy^+} - \overline{v^+\theta^+} = -1. \quad (6)$$

The simulation of Lyons *et al.* [4] is in this category. The present experiments should also belong to this case provided the length of the heated wall is sufficiently large for the constant temperature boundary condition to become a reasonable approximation to a constant heat flux boundary.

Case b: $A = 1$

Both walls are heated at the same constant heat flux. From equation (5), $Q = -q_w/\delta$, so that a heat sink is rquired to maintain $d\bar{T}/dx = 0$. The total heat flux varies linearly, i.e.

$$Pr^{-1}\frac{d\bar{T}^+}{dy^+} - \overline{v^+\theta^+} = \frac{y^+}{\delta^+} - 1. \quad (7)$$

The simulation of Kim and Moin [3] belongs to this category provided q_w is negative. The two walls are therefore cooled at the same rate and Q represents an internal heat source. Kasagi *et al.*'s [5] simulation would belong to this category except that Q is zero so that $\bar{T}_w$ and the bulk mean temperature increase linearly with x.

Case c: $A = 0$

Wall 2 is adiabatic and a sink $Q = -q_w/2\delta$, equal to half the value in case b, is required. The variation in the total heat flux is linear, namely

$$Pr^{-1}\frac{d\bar{T}^+}{dy^+} - \overline{v^+\theta^+} = \frac{y^+}{2\delta^+} - 1. \quad (8)$$

The Reynolds number δ^+ appears explicitly in equations (7) and (8) but is absent in equation (6). One may surmise that the effect of Reynolds number on $\overline{v^+\theta^+}$ may be different for case a than in cases b and c, even though the influence of δ^+ on the Reynolds stresses should be identical in the three cases. It is therefore of interest to consider the dependence of $-\overline{v^+\theta^+}(d\bar{T}^+/dy^+)$ on δ^+.

Equations (6)–(8) allow $\overline{v^+\theta^+}$ to be expressed in terms of $d\bar{T}^+/dy^+$, Pr and δ^+. It is easy to show that in all three cases, the maximum value of $-\overline{v^+\theta^+}(d\bar{T}^+/dy^+)$ is given by

$$\left(-\overline{v^+\theta^+}\frac{d\bar{T}^+}{dy^+}\right)_{max} = \frac{Pr}{4} \quad (9)$$

and occurs when

$$\frac{d\bar{T}^+}{dy^+} = -\frac{Pr}{2}, \quad \overline{v^+\theta^+} = \tfrac{1}{2}. \quad (10)$$

In case a, equation (9) is valid regardless of the actual value of δ^+. In cases b and c, equation (9) is correct only when $\delta^+ \to \infty$. It seems therefore possible that the dependence of $\overline{v^+\theta^+}$ and $-\overline{v^+\theta^+}(d\bar{T}^+/dy^+)$ on the Reynolds number may depend on the nature of the thermal boundary conditions that are used.

3. EXPERIMENTAL CONDITIONS

Measurements were carried out in a fully developed turbulent duct flow over a range of Reynolds numbers ($Re = U_0\delta/\nu$) = 3300 to 10650, where δ is 21 mm. The majority of the detailed data were taken at $Re = 3300$ ($\delta^+ = 181$), which is approximately the value for which the DNS data were obtained. The duct aspect ratio of 18 and the measurement locations ($x/\delta > 250$, x is measured from the entrance to the working section) were sufficiently large to ensure a fully developed two-dimensional mean flow. Experimental evidence in support of a fully developed flow was given in ref. [8].

The duct walls were made of aluminium and perspex, respectively. The aluminium wall (1.27 cm thick) consisted of four plates, each of which could be heated separately by Sierracin pads (0.1 mm thick) connected in series and arranged in two rows of six along the length of each plate. The pads are bonded to the backs of the plates, thermal insulation (45 mm thick) ensuring that the heat loss from the backs is small. The amount of heat supplied to each plate was controlled and the temperature of the entire wall was continuously monitored using integrated-circuit temperature transducers embedded in small holes (using a highly conductive silicone compound) drilled at many x and z locations in the backs of the plates. The perspex wall was sufficiently thick (19 mm) to represent a reasonable approximation to a constant temperature boundary condition. The temperature of the inner surface of the perspex wall was 0.5°C higher than the ambient temperature of the outer surface. This temperature difference, which resulted in a heat flux nearly equal to that of the aluminium wall, explains why a heat sink was not required to achieve a thermally fully developed flow.

The complete length of the aluminium wall was heated, the wall temperature being homogeneous in the streamwise and spanwise directions to within an uncertainty of ±3%. The temperature difference between the heated wall and ambient temperature was maintained at about 10°C and the other (perspex) wall was at approximately ambient temperature. Measurements were made at $x/\delta = 279$ and 308.

Measurements were made with a single cold wire (1.2 mm long, 1.27 μm diameter Pt–10% Rh) which was operated in a constant current (50 μA) circuit and traversed across the duct with a mechanism with a least count of 0.01 mm. The initial distance of the wire from the wall was determined using the reflection method and a theodolite. A d.c. offset voltage was applied to the signal from the constant current circuit before it was amplified and low-pass filtered at a cut-off frequency of 1.75 kHz. The signal was then digitized on a personal computer using a 12 bit A/D converter at a sampling frequency of 3.5 kHz. The data was then transferred (using an ETHERNET optical link) to a 780 VAX cluster for subsequent analysis.

To assess the influence of Reynolds number on the mean and fluctuating temperature in the near-wall region, measurements were made at three values of Re (3300, 6800, 10 650). A 0.63 μm diameter cold wire made of the same material and operated under the same conditions as the 1.27 μm wire was used. The wire was bent (before etching) into a U-shape to allow measurements to be made very close to the wall. In all cases, the wall heat flux q_w was estimated (to an accuracy of $\pm 5\%$) from the slope of the mean-temperature profile in the region $y^+ \leqslant 6$.

4. RESULTS AND DISCUSSION

Mean temperature profiles at $x/\delta = 279$ and 308 are compared in Fig. 2 with the DNS results reported in refs. [3, 4]. The good agreement between the measured distributions at the two x stations is consistent with the expectation of a thermally fully developed flow. The value of q_w was the same at both stations, confirming a constant heat flux boundary condition. For $y^+ < 40$, the agreement between experiment and DNS is good (Fig. 2) despite the different thermal boundary conditions for each set of data. The agreement is even better for $y^+ < 10$. In the region $40 < y^+ < 180$, the magnitude of $d\bar{T}^+/dy^+$ increases for the experiment and ref. [4] but decreases near the duct centreline for refs. [3, 5]. This behaviour is expected in the DNS results of refs. [3, 5] since both walls were either heated or cooled, so that the gradient should be zero at the centre of the duct. In the experiment and in the simulation of ref. [4] where one wall is heated and the other cooled, the mean temperature gradient at the centre of the channel is, as expected, non-zero. The ratio $\bar{T}^+/Pr$ has been plotted in Fig. 2 since $\bar{T}^+ \to Pr\,y^+$ as $y^+ \to 0$. With this presentation, the $Pr = 1$ distribution of ref. [4] is in reasonable agreement near the wall with all other distributions ($Pr = 0.71$).

The r.m.s. distributions of the temperature θ'^+ are shown in Fig. 3 and compared to the DNS results. The agreement between the measured profiles at the two x stations gives further support for the assumption of thermally fully developed flow. Small deviations between the two sets of results are within the experimental uncertainty ($\pm$ 2%). It is expected that all the DNS results will be in close agreement with each other and with the experimental results close to wall 1, since the boundary conditions at this wall are similar (i.e. heat is either introduced or removed at a constant rate). Indeed, the agreement between experiment and DNS is quite good when $y^+ < 40$. The effect of the thermal boundary condition at wall 2 on the mean and fluctuating temperature is observed for $y^+ \gtrsim 40$. In the case of $\bar{T}^+$ (Fig. 2), the agreement between experiment and DNS is improved for $y^+ < 10$. It is easy to show that, in the limit of $y^+ \to 0$, $\theta'^+ = \beta y^+ + O(y^{+3})$. Using the near-wall DNS data, Antonia and Kim [9] found that $\beta \sim Pr$, at least for $Pr = 0.71$ and 2, the constant of proportionality having a value of about 0.36 (the same value as that of the first coefficient in the near-wall expansion of u'^+). The use of θ'^+/Pr in Fig. 3 shows that there is indeed agreement between Lyons *et al.* ($Pr = 1$) data and the other data ($Pr = 0.71$) at small y^+. There is also reasonable agreement with $\theta'^+/Pr = 0.36y^+$. Among the four sets of data presented in Fig. 3, it appears that, for $y^+ > 60$, the normalized temperature variance is largest for ref. [4] (one wall heated and the other cooled at the same rate; the mean temperature profile is symmetrical about the centreline). For ref. [4], the variance increases continuously towards the centreline, reaching a maximum of about 3.5 at $y = \delta$. For the boundary conditions of ref. [3], θ'^+/Pr decreases monotonically towards the centreline to a minimum of about 1. It appears that their results represent the case for which θ'^+/Pr has the lowest values everywhere in the considered region. A similar behaviour is observed in the data of ref. [5]. In the present experiment, the distribution is approximately constant in the region $70 < y^+ < 110$ and decreases rapidly to about 2 near the centreline.

A least squares cubic-spline was used to provide a fit to the measured mean temperature profile. The best fit profile was then differentiated to form $d\bar{T}^+/dy^+$. The heat flux $\overline{v^+\theta^+}$ was calculated from equation (6)

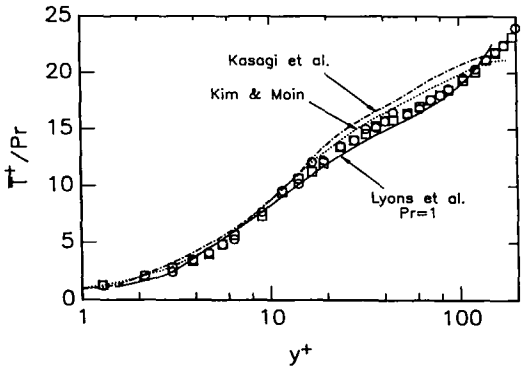

FIG. 2. Mean temperature distribution. Present experiment: □, $x/\delta = 279$; ▽, 308. DNS: – – –, Kim and Moin [3]; – · – · –, Kasagi *et al.* [5]; ——, Lyons *et al.* [4].

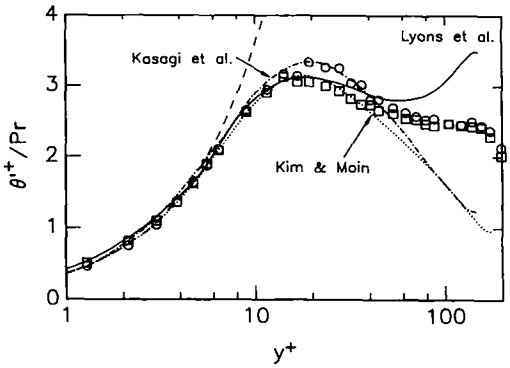

FIG. 3. R.m.s. temperature distribution. Present experiment: □, $x/\delta = 279$; ▽, 308. DNS: – – –, ref. [3]; – · – · –, ref. [5]; ——, ref. [4]. — —, $\theta'^+/Pr = 0.36y^+$.

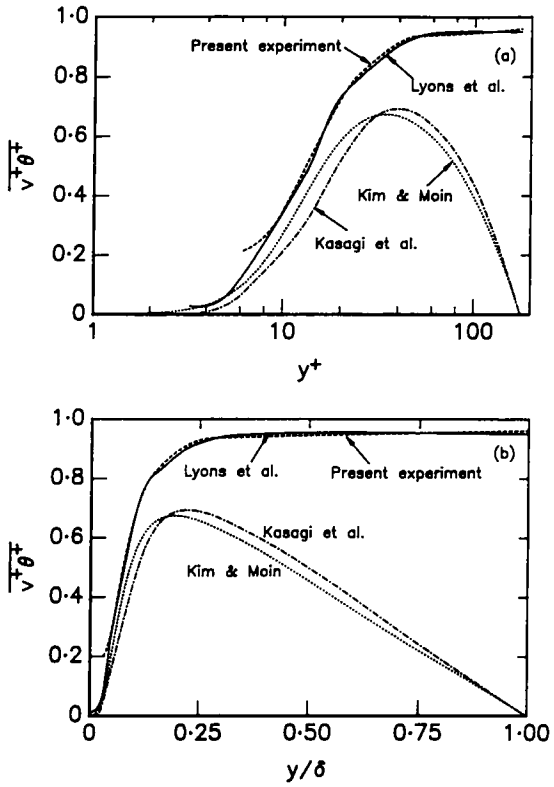

FIG. 4. Heat flux distributions. Present experiment: ---, using mean temperature profile and equation (6). DNS: ——, ref. [4]; · · · · ·, ref. [3]; -·-·-, ref. [5]. (a) $\overline{v^+\theta^+}$ vs y^+; (b) $\overline{v^+\theta^+}$ vs y/δ.

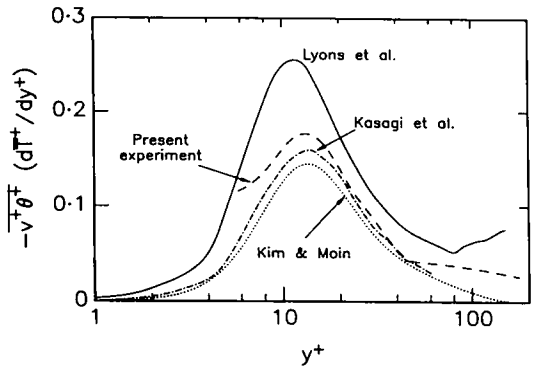

FIG. 5. Distribution of average production of temperature variance. Present experiment: ---. DNS: ——, ref. [4]; · · · · ·, ref. [3]; -·-·-, ref. [5].

and the previously obtained $d\bar{T}^+/dy^+$ and plotted in Figs. 4(a) and (b). There is good agreement between our results and those of ref. [4]. The poor agreement in the region $y^+ < 9$ as seen in Fig. 4(a) is due to the inaccuracy in $d\bar{T}^+/dy^+$ for this region. Whereas $\overline{v^+\theta^+}$ varies linearly with y/δ for refs. [3, 5], it is nearly constant (for $y/\delta > 0.25$) for our case and ref. [4] (Fig. 4(b)). From Fig. 4(a), it appears that the effect of the different boundary condition at wall 2 can be observed at a small distance ($y^+ \simeq 6$) from wall 1. The effect is mainly observed in the region $y^+ > 40$ as in the case of T^+/Pr and θ'^+/Pr. Although the boundary condition at wall 1 is similar in all cases (i.e. constant heat flux) the distribution of $\overline{v^+\theta^+}$ near that wall depends strongly on the boundary condition at the opposite wall.

Once the heat flux $\overline{v^+\theta^+}$ is known, the turbulent production term $-\overline{v^+\theta^+}(d\bar{T}^+/dy^+)$ can be calculated (Fig. 5). This term has a peak at approximately $y^+ = 12$, independently of the boundary condition at wall 2. Its magnitude depends on the Reynolds number when boundary conditions similar to those of ref. [3] or ref. [5] are applied but is Reynolds number independent for boundary conditions similar to those of ref. [4] and the present experiment. As shown previously, this term has a maximum value equal to $Pr/4$, i.e. 0.178 when $Pr = 0.71$. Near the channel centreline, this term seems to be very dependent on the boundary condition of wall 2. While it is equal to zero in ref. [3], it has a value of 0.075 in ref. [4] and 0.027 in the present results. As pointed out in ref. [4], the reason for this behaviour is the significant gradient of temperature that exists near the centreline of the duct when heat is introduced at one wall and removed at the other. The relatively high value of production near the centre of the duct is consistent with the large value of θ'^+ there (in ref. [4] the channel centreline is at $y^+ = 150$ while in our experiment and ref. [3], it is at $y^+ \approx 180$).

The present values of the Stanton number St and the Reynolds analogy factor ($2St/C_f$) are 3.32×10^{-3} and 1.14, respectively. The latter value is in good agreement with that obtained from the Prandtl–Taylor analogy (e.g. p. 437 of ref. [7]) when a 'global' value for Pr_T is taken as 0.9 (a value generally used in wall-bounded flows). The present Nusselt number Nu is 15.4, in good agreement with ref. [5], but smaller than the value (25.36) reported in ref. [4], apparently due to the higher Prandtl number ($Pr = 1$) used in that simulation.

Mean and fluctuating temperatures, shown in Figs. 6 and 7 respectively, were measured at three different Reynolds numbers, $Re = 3300$, 6800 and 10 650. Most

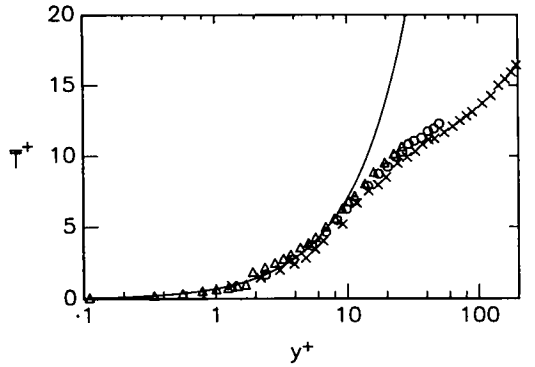

FIG. 6. Mean temperature distribution in near-wall region. ×, $Re = 3300$; ○, $Re = 6800$; △, $Re = 10650$; ——, $\bar{T}^+ = Pr\,y^+$.

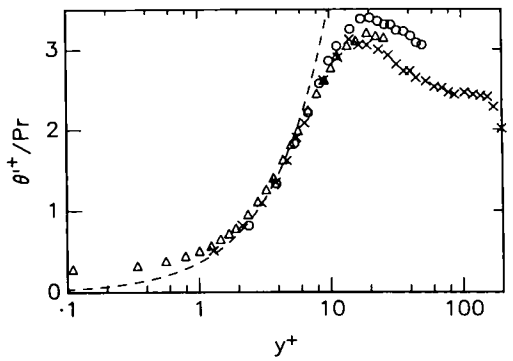

FIG. 7. R.m.s. temperature distribution in near-wall region. ×, $Re = 3300$; ○, $Re = 6800$; △, $Re = 10650$; ——, $\theta'^+/Pr = 0.36y^+$.

of the measurements were made in the near-wall region, as a significant Reynolds number dependence of the velocity field has been found in this region. Although the DNS data show that the r.m.s. velocity is Reynolds number dependent in the region $y^+ < 10$ [10], the present experimental data for θ'^+ do not show a Reynolds number dependence, allowing for an estimated uncertainty of $\pm 2\%$. It may, however, also be related to the present thermal boundary conditions and the fact that $-\overline{v^+\theta^+}(d\bar{T}^+/dy^+)$ is independent of Re. Figures 6 and 7 suggest that the mean and r.m.s. temperature distributions collapse in the region $y^+ < 10$ for the present Reynolds number range. For $y^+ \lesssim 6$, Fig. 7 shows reasonable agreement between the measured r.m.s. temperature and the relation $\theta'^+ = 0.36Pr\,y^+$.

5. CONCLUSIONS

(1) The experimental situation in which the complete length of one of the duct walls is slightly heated at constant temperature represents a good approximation to a constant heat flux boundary, when measurements are carried out at a sufficiently large distance from the heating origin. In the present experiment, this distance exceeds 270δ and the flow can be assumed to be thermally fully developed (provided wall 2 is at approximately ambient temperature).

(2) The mean and r.m.s. temperature are strongly affected by the boundary condition at wall 2 in the region $y^+ \gtrsim 40$. The effect is negligible for $y^+ < 10$, where there is good agreement between experiment and simulations.

(3) The maximum value of the production of temperature variance $-\overline{v^+\theta^+}(d\bar{T}^+dy^+)$ depends on the Prandtl number (and not on the Reynolds number) for a fully developed thermal flow with one wall heated and the other cooled (at the same rate). When both walls are heated, this maximum value increases with the Reynolds number.

(4) In the region $y^+ > 40$, the heat flux $\overline{v^+\theta^+}$ depends strongly on the boundary condition at wall 2 but there is no significant Prandtl number effect.

(5) The mean and r.m.s. temperature distributions appear to be independent of the Reynolds number in the region $y^+ < 10$.

Acknowledgement—The support of the Australian Research Council is gratefully acknowledged.

REFERENCES

1. J. Kim, P. Moin and R. Moser, Turbulence statistics in fully developed channel flow at low Reynolds number, *J. Fluid Mech.* **177**, 133–166 (1987).
2. J. Kim, Investigation of heat and momentum transport in turbulent flows via numerical simulations. In *Transport Phenomena in Turbulent Flows* (Edited by M. Hirata and N. Kasagi), pp. 715–730. Hemisphere, New York (1988).
3. J. Kim and P. Moin, Transport of passive scalars in a turbulent channel flow. In *Turbulent Shear Flows 6*, pp. 85–96. Springer, Berlin (1989).
4. S. L. Lyons, T. M. Hanratty and J. B. McLaughlin, Direct numerical simulation of passive heat transfer in a turbulent channel flow, *Int. J. Heat Mass Transfer* **34**, 1149–1161 (1991).
5. N. Kasagi, Y. Tomita and A. Kuroda, Direct numerical simulation of the passive scalar field in a two-dimensional channel flow, to be presented at *3rd ASME–JSME Thermal Engng Joint Conf.*, Reno (1991).
6. F. M. White, *Heat and Mass Transfer*. Addison-Wesley, New York (1988).
7. V. S. Arpaci and P. S. Larsen, *Convection Heat Transfer*. Prentice-Hall, Englewood Cliffs, New Jersey (1984).
8. M. Teitel and R. A. Antonia, The interaction region in a turbulent duct flow, *Physics Fluids A* **2**, 808–813 (1990).
9. R. A. Antonia and J. Kim, Turbulent Prandtl number in the near-wall region of a turbulent channel flow, *Int. J. Heat Mass Transfer* **34**, 1905–1908 (1991).
10. R. A. Antonia, M. Teitel, J. Kim and L. W. B. Browne, Low Reynolds number effects in a fully developed turbulent duct flow, *J. Fluid Mech.* **236**, 579–605 (1992).